MNRAS **000**, 000–000 (0000) Preprint 1 March 2016 Compiled using MNRAS LATEX style file v3.0

Global diffusion of cosmic rays in random magnetic fields

A. P. Snodin,[1,2] ⋆ A. Shukurov,[3] G. R. Sarson,[3] P. J. Bushby[3] and L. F. S. Rodrigues[3]

[1]*Department of Materials and Production Technology Engineering, Faculty of Engineering, King Mongkut's University of Technology North Bangkok, Bangkok 10800, Thailand*
[2]*Department of Mathematics, Faculty of Applied Science, King Mongkut's University of Technology North Bangkok, Bangkok 10800, Thailand*
[3]*School of Mathematics and Statistics, Newcastle University, Newcastle upon Tyne, NE1 7RU, U.K.*

1 March 2016

ABSTRACT

The propagation of charged particles, including cosmic rays, in a partially ordered magnetic field is characterized by a diffusion tensor whose components depend on the particle's Larmor radius $R_{\rm L}$ and the degree of order in the magnetic field. Most studies of the particle diffusion presuppose a scale separation between the mean and random magnetic fields (e.g., there being a pronounced minimum in the magnetic power spectrum at intermediate scales). Scale separation is often a good approximation in laboratory plasmas, but not in most astrophysical environments such as the interstellar medium (ISM). Modern simulations of the ISM have numerical resolution of order 1 pc, so the Larmor radius of the cosmic rays that dominate in energy density is at least 10^6 times smaller than the resolved scales. Large-scale simulations of cosmic ray propagation in the ISM thus rely on oversimplified forms of the diffusion tensor. We take the first steps towards a more realistic description of cosmic ray diffusion for such simulations, obtaining direct estimates of the diffusion tensor from test particle simulations in random magnetic fields (with the Larmor radius scale being fully resolved), for a range of particle energies corresponding to $10^{-2} \lesssim R_{\rm L}/l_{\rm c} \lesssim 10^3$, where $l_{\rm c}$ is the magnetic correlation length. We obtain explicit expressions for the cosmic ray diffusion tensor for $R_{\rm L}/l_{\rm c} \ll 1$, that might be used in a sub-grid model of cosmic ray diffusion. The diffusion coefficients obtained are closely connected with existing transport theories that include the random walk of magnetic lines.

Key words: magnetic fields – diffusion – MHD – turbulence – methods: numerical – cosmic rays

1 INTRODUCTION

The theory of propagation and confinement of cosmic rays is largely based on analytical calculations (mostly quasilinear, applicable if magnetic fluctuations are much weaker than the background magnetic field) of the scattering of charged relativistic particles by magnetic inhomogeneities (Berezinskii et al. 1990; Schlickeiser 2002; Kulsrud 2004; Strong et al. 2007). Analytical results have been verified and extended by simulations of the motion of test particles (Giacalone & Jokipii 1994, 1999; Casse et al. 2001; Candia & Roulet 2004; Plotnikov et al. 2011) in model magnetic fields $\boldsymbol{B}$ represented as the sum of a mean field $\boldsymbol{B}_0$ and fluctuations $\boldsymbol{b}$,

$$\boldsymbol{B} = \boldsymbol{B}_0 + \boldsymbol{b}\,. \tag{1}$$

The main goal of the test particle simulations has been the verification of the analytical results and their extension, especially to the case of finite magnetic fluctuations (e.g., Shalchi & Dosch 2009), often focusing on the dependence of the cosmic ray propagation parameters on the particle energy.

The results are formulated in terms of the cosmic ray diffusion tensor

$$K_{ij} = K_\perp \delta_{ij} + (K_\parallel - K_\perp)\widehat{B}_i \widehat{B}_j\,, \tag{2}$$

where $\widehat{\boldsymbol{B}} = \boldsymbol{B}/|\boldsymbol{B}|$ is the unit vector in the magnetic field direction, and $K_\parallel$ and $K_\perp$ are, respectively, the cosmic ray diffusivities along and across the mean magnetic field (e.g., Giacalone & Jokipii 1999, and references therein). Extensive numerical results have been obtained for a wide range of the particle rigidity, $10^{-2} \lesssim \rho \lesssim 10^3$, where

$$\rho = R_{\rm L}/l_{\rm c} \approx E/q\,,$$

with

$$R_{\rm L} \approx 3.3 \times 10^{12}{\rm cm} \left(\frac{B}{1\,\mu{\rm G}}\right)^{-1} \left(\frac{E}{1\,{\rm GeV}}\right) \sin\theta \tag{3}$$

the Larmor radius of the particle's gyration in the magnetic field (here given for ultra-relativistic protons), $l_{\rm c}$ the correlation length

⋆ E-mail: andrew.snodin@gmail.com; anvar.shukurov@ncl.ac.uk; g.r.sarson@ncl.ac.uk; paul.bushby@ncl.ac.uk; luiz.rodrigues@ncl.ac.uk

of magnetic fluctuations, E and q the total particle energy and electric charge, and θ the angle between the magnetic field and the particle velocity (the pitch angle). The results of test particle simulations are in approximate agreement with theoretical estimates and can be fitted with the form (Section 2.3 of Strong et al. 2007)

$$K_{\parallel} = \kappa_0 \left(\frac{E}{1\,\mathrm{GeV}} \right)^n \frac{B_0^2}{b_0^2}\,, \tag{4}$$

with an accompanying expression for $K_{\parallel}/K_{\perp}$, where b_0 is the root-mean-square strength of magnetic fluctuations, $n = 1/3$–$1/2$ depending on the magnetic power spectrum, and $\kappa_0 \simeq (3\text{–}5) \times 10^{28}\,\mathrm{cm^2\,s^{-1}}$ for the Galactic cosmic rays near the Sun. The spectrum of magnetic fluctuations in the ISM extends from the outer scale of order 100 pc[1] apparently down to at least 10^6 cm (Armstrong et al. 1995). Therefore, the Larmor radius of cosmic ray particles of GeV energies is well within the range of magnetic turbulent scales.

The diffusion of charged particles in a random magnetic field is a result of two dominant effects. Particles gyrating in a magnetic field are scattered by magnetic fluctuations — which may be part of the externally driven magnetic spectrum or be self-generated by the streaming instability (Kulsrud 2004) — at a scale comparable to R_{L}. Due to the scattering, the particle propagation both along and across the magnetic field becomes diffusive. The divergence of the field lines of a random magnetic field that guides the particles further enhances their diffusion. As a result, the propagation of cosmic rays is sensitive to both local and global properties of the magnetic field. Sonsrettee et al. (2015b) present a detailed analysis of the random walk of magnetic lines with vanishing mean magnetic field (see also Snodin et al. 2013; Sonsrettee et al. 2015a).

The dominant contribution to the scattering of charged particles is provided by resonant magnetic fluctuations at a scale close to the particle's Larmor radius given by Equation (3). Magnetic fluctuations at such a small scale can be measured or estimated only in rare cases, e.g., *in situ* in the interplanetary space. This makes it difficult to apply the theory of cosmic ray diffusion to interstellar or intergalactic cosmic rays at their dominant energies, $E \simeq (1\text{–}10) \times 10^3$ GeV per nucleon, since little beyond crude statistical properties of random magnetic fields at their outer (or energy-range) scale is known with any degree of confidence. This scale is of the order of 3×10^{20} cm (100 pc) in the interstellar space and 3×10^{22} cm (10 kpc) in galaxy clusters, by far larger than the resonant scale of the cosmic ray particles.

More importantly, models of cosmic ray propagation rely on the representation (1) for magnetic field, which is meaningful and useful only in the case of a clear scale separation between the mean magnetic field and its fluctuations. Under such a scale separation, the range of scales (spatial and/or temporal) over which the mean magnetic field varies is clearly distinct from that of the random magnetic field; we note that the mean magnetic field does not need to be uniform (Gent et al. 2013; Farge & Schneider 2015). For example, scale separation can manifest itself as a local minimum in the magnetic power spectrum at a scale larger than the outer turbulent scale (see Gent et al. 2013, for a discussion). Clear separation of the mean magnetic field and fluctuations is typical of laboratory plasmas and the solar wind (Goldstein et al. 1995; Howes 2015), where the mean and fluctuating magnetic fields vary in space and time at widely separated scales. However, there are neither theoretical nor observational reasons to expect that the spectra of interstellar or intergalactic magnetic fields would have such a feature. In any event, the existence of such a separation at a scale comparable to a certain value of R_{L} would justify Equation (1) only over a relatively narrow range of particle energies, rather than for the wide range of R_{L} required in a propagation model. A consistent interpretation of Equation (4) could be to use it as a scale-dependent diffusivity with the scale-dependent 'mean' magnetic field defined as $B_0^2(k) = \int_0^k b^2(k')\,\mathrm{d}k'/k'$ or similarly, but then the propagation of cosmic rays has to be described with an integral equation which can be reduced, under certain conditions, to a partial differential equation of a more complicated form than the diffusion equation (e.g., Section 5.4 in Bakunin 2008, see also Snodin et al. (2006)).

As a result, large-scale simulations of cosmic ray propagation in the galaxies use the forms (2) and (4), or even a scalar diffusivity with κ_0 simply taken to be constant or a heuristic function of position designed to model galactic spiral arms, disc and halo. This is true even of such advanced cosmic ray modelling tools as the GALPROP (Strong & Moskalenko 2001; Strong et al. 2007; Vladimirov et al. 2011), COSMOCR (Miniati 2001) and DRAGON (Evoli et al. 2008; Gaggero et al. 2013; Maccione 2013) codes; see also Miniati (2007); Hanasz et al. (2009); Siejkowski et al. (2014). This is an oversimplification since both parameters that control cosmic ray diffusion, the ratio of the Larmor radius to the turbulent correlation scale and the strength of magnetic fluctuations, depend on all MHD variables including gas density, velocity and temperature. As a result, the relation of the local energy density of cosmic rays to the ISM parameters, a question of primary importance in radio astronomy, remains uncertain (e.g., Stepanov et al. 2014, and references therein).

One of the goals of this paper is to develop approaches to a more physically detailed modelling of cosmic ray propagation in numerical magnetohydrodynamic (MHD) simulations of the interstellar medium (ISM). Since the Larmor radius of cosmic ray particles is by far smaller than the numerical resolution of any ISM simulations, which tend to resolve scales down to the order of a parsec, a subgrid model of cosmic ray diffusion is required. Most test-particle simulations of cosmic ray diffusion in the context of the ISM employ a synthetic random magnetic field specified in continuous space, as in Equation (9) below (see, however, Casse et al. 2001; De Marco et al. 2007; Beresnyak et al. 2011), whereas the ISM simulations use a numerical grid with a certain spatial resolution. This should not prevent such results from being used in grid-based simulations, but we consider test particles motion in both continuous and discrete spatial domains in Section 2.1 to appreciate their limitations and select optimal parameter ranges.

Analytical studies of the propagation of charged particles in random magnetic fields have produced deep insights (see Casse et al. 2001, for a useful review), many of which show consistency with test particle simulations. However, such analytical results are not particularly accurate over a wide range of parameters, presumably due to the assumptions involved in their derivation. Here we adopt an empirical approach and aim at deriving approx-

[1] This estimate of the largest scale in the interstellar inertial range follows from analyses of the interstellar velocity field (page 148 in Ruzmaikin et al. 1988, and references therein). Observations of interstellar turbulence in various tracers, e.g., Faraday rotation (Minter & Spangler 1996) or fluctuations of synchrotron intensity (Haverkorn et al. 2008; Iacobelli et al. 2013), which depend on products of fluctuating quantities, unsurprisingly suggest smaller values of the turbulent scale as long as they are not interpreted in terms of the statistical properties of each of the physical variables involved (thermal and cosmic-ray electron densities, magnetic field, etc.) (Stepanov et al. 2014). Such an interpretation is hampered by the fact that the variables can be correlated or anticorrelated to a poorly known degree (Beck et al. 2003; Stepanov et al. 2014).

imate asymptotic forms of the diffusion tensor from test particle simulations, which may be useful in a wide range of applications. The studies of cosmic ray propagation with test particles often focus on energetic particles whose Larmor radius is comparable to or exceeds the correlation length of magnetic fluctuations. However, a sub-grid model of cosmic ray diffusion requires the opposite limit, of a Larmor radius much smaller than the scales at which magnetic field is known. This limiting case is our main concern in this paper: we attempt to develop expressions for the cosmic ray diffusion tensor in a partially ordered, random magnetic field that can be extrapolated to scales much larger than the particles' Larmor radius. Thus, in order to deduce the limiting behaviour, we perform test particle simulations in magnetic fields containing a large range of scales, but where the particle Larmor radius is well resolved numerically and is smaller than the correlation length of the magnetic field. The obtained components of the cosmic ray diffusion tensor can then be applied to much larger scales, depending on the particle momentum and the magnetic field strength on those scales.

2 TEST PARTICLE SIMULATIONS

Most test particle simulations employ a synthetic random magnetic field, either composed of a superposition of static plane waves or specified on a discrete mesh. Earlier simulations have demonstrated that the propagation of charged particles in a random magnetic field is very sensitive to subtle details of the magnetic field structure, such as the density at which the wave vector space is populated with magnetic modes and the range of wave numbers involved, etc. (Casse et al. 2001; Parizot 2004; Fatuzzo et al. 2010; Plotnikov et al. 2011). Here we describe test particle simulations in which two quite different models of an isotropic turbulent magnetic field are used and carefully compared in order to better understand these subtleties. The magnetic fields are taken to be stationary. We neglect electric fields since they are expected to have a negligible effect on relativistic particle energy as the acceleration time is likely to be much greater than the diffusion time (Fatuzzo et al. 2010).

In one model used here, the magnetic field is defined at the particle's location using an explicit algebraic expression. The other model constructs the magnetic field on a regular mesh, as in MHD simulations. Equations of motion are then solved for a large number of particles of a given Larmor radius, over a number of magnetic field realisations. The elements of the diffusion tensor are then obtained as functions of time from the mean-squared particle displacements, with averaging over the particle trajectories and magnetic field realisations. At a suitably large time, where the diffusion coefficients have settled to steady values, asymptotic diffusion coefficients can be obtained.

Our model magnetic field is of the form (1) where $\boldsymbol{B}_0 = B_0\hat{\boldsymbol{z}}$ is a uniform mean field and $\boldsymbol{b}$ is a random component, with $\langle \boldsymbol{b} \rangle = \boldsymbol{0}$ (where angular brackets denote suitable averaging). It is convenient to parameterize the turbulence level with

$$\eta = \frac{b_0^2}{b_0^2 + B_0^2}\,, \tag{5}$$

where $0 \le \eta \le 1$ and $b_0^2 = \langle \boldsymbol{b}^2 \rangle$; we note that $(b_0/B_0)^2 = \eta/(1-\eta)$. Here $\eta = 0$ corresponds to a uniform, unperturbed magnetic field, whilst $\eta = 1$ implies no mean field, with the magnetic field being dominated by turbulent small-scale components. The random magnetic field is assumed to have an isotropic power spectrum

$$M(k) = M_0 \begin{cases} 0 & \text{for } k < k_0, \\ (k/k_0)^{-s} & \text{for } k \ge k_0, \end{cases} \tag{6}$$

where M_0 is a normalization constant related to the desired turbulent magnetic energy density b_0^2, and $k_0 = 2\pi/L$, with L the largest (outer) scale of turbulence. Therefore, the spectral power of the magnetic field is localised at well-separated wave numbers, $k \ge k_0$ due to the random field, and $k = 0$ due to the mean (in this case, uniform) part.

We consider two values of the spectral index, $s = 5/3$ or $3/2$, to explore its effects on the particle transport. The correlation length l_c of an isotropic field is given by (Monin & Yaglom 1975)

$$l_c = \frac{\pi}{2} \frac{\int_0^\infty k^{-1} M(k)\,\mathrm{d}k}{\int_0^\infty M(k)\,\mathrm{d}k}\,, \tag{7}$$

with $l_c = 0.1L = \pi/(5k_0)$ for $s = 5/3$, and $l_c = \pi/(6k_0)$ for $s = 3/2$. Our numerical implementations of the random magnetic field have discrete values of the wave number k and extend to some maximum $k = k_{\max}$. As a result, the effective value of the correlation length differs by up to a few per cent from the above values obtained for $k_{\max} \to \infty$. We also considered a magnetic spectrum of the form

$$M(k) = M_0 \frac{(k/k_b)^4}{[1 + (k/k_b)^2]^{s/2+2}}\,, \tag{8}$$

which is similar to Equation (6), but has the peak in the energy spectrum near some chosen k_b rather than at k_0.

2.1 Magnetic field models

The first approach is to represent the magnetic field as a sum of a finite number of plane-wave modes with random polarizations, wave vectors and phases. It can be shown (e.g., Batchelor 1953) that the resulting field is spatially homogeneous and isotropic in the limit of an infinite number of modes. Giacalone & Jokipii (1994) implemented this idea which has subsequently been used in many studies involving test particle simulations. Here we use a very similar method based on a time-independent version of the velocity field used by Fung et al. (1992) to model synthetic turbulence (and often used in modelling of turbulent flows by other authors). We take

$$\boldsymbol{b}(\boldsymbol{x}) = \sum_{n=1}^{N} \left[\boldsymbol{C}_n \cos(\boldsymbol{k}_n \cdot \boldsymbol{x}) + \boldsymbol{D}_n \sin(\boldsymbol{k}_n \cdot \boldsymbol{x})\right], \tag{9}$$

where $\boldsymbol{k}_n$ are randomly oriented wave vectors, and $\boldsymbol{C}_n$ and $\boldsymbol{D}_n$ are random vectors confined to the plane perpendicular to $\boldsymbol{k}_n$ to ensure that $\nabla \cdot \boldsymbol{b} = 0$. With

$$|\boldsymbol{C}_n|^2 = |\boldsymbol{D}_n|^2 = \frac{\Delta k_n M(k_n)}{\sum_{n=1}^{N} \Delta k_n M(k_n)}, \tag{10}$$

where Δk_n is a suitable wave number spacing as defined below, the desired energy spectrum is obtained. The random angle between the amplitude vectors controls the random polarization of the plane waves. An efficient way to model a power-law spectrum is to select geometrically spaced wave numbers k_n between k_0 and $k_{\max}$:

$$k_n = k_0 \left(\frac{k_N}{k_0}\right)^{(n-1)/(N-1)}\,, \tag{11}$$

where $1 \le n \le N$ (so that $k_1 = k_0$ and $k_N = k_{\max}$). In Equation (10), we then take $\Delta k_1 = (k_2 - k_1)$, $\Delta k_N = (k_N - k_{N-1})$, and otherwise $\Delta k_n = (k_{n+1} - k_{n-1})/2$, for $2 \le n \le N-1$. For large N, the resulting magnetic field is essentially non-periodic, which is potentially useful in detecting periodicity effects when compared with the second (periodic) model described below. An appropriate value for N depends on the context; we examine this in

Appendix A. This model of a random magnetic field will be henceforth referred to as the *continuum model*.

The second model implements a spatially periodic random magnetic field on a regular, three-dimensional Cartesian mesh, similarly to Casse et al. (2001). First, a regular grid in the three-dimensional wave number space is populated with complex Fourier components $\boldsymbol{b}(\boldsymbol{k})$ given by

$$\boldsymbol{b}(\boldsymbol{k}) = A(k)[\boldsymbol{b}_1(\boldsymbol{k})e^{\mathrm{i}\phi_1(\boldsymbol{k})} + \mathrm{i}\boldsymbol{b}_2(\boldsymbol{k})e^{\mathrm{i}\phi_2(\boldsymbol{k})}], \tag{12}$$

where $\boldsymbol{b}_1$ and $\boldsymbol{b}_2$ are random, real unit vectors perpendicular to both $\boldsymbol{k}$ (to ensure that $\nabla \cdot \boldsymbol{b} = 0$) and each other, so that $\boldsymbol{b}_1$ is chosen at random and $\boldsymbol{b}_2 = \widehat{\boldsymbol{k} \times \boldsymbol{b}_1}$, where the hat denotes a unit vector. Here $\phi_1(\boldsymbol{k})$ and $\phi_2(\boldsymbol{k})$ are distinct random phases that control the polarization of the magnetic field modes. We note that results presented below, at least for $\eta = 1$, are not particularly sensitive to the random phases, and taking $\phi_1(\boldsymbol{k}) = \phi_2(\boldsymbol{k}) = 0$ changes the results very little: the randomness in the choice of $\boldsymbol{b}_1$ is sufficient to ensure randomness in the relative phases of different modes. We take $A(k) \propto \sqrt{M(k)}/k$ to set the correct energy spectrum. We enforce Hermitian symmetry on $\boldsymbol{b}(\boldsymbol{k})$ so that the inverse Fourier transform of Equation (12) yields a real, random magnetic field which we then normalise to the desired energy density b_0^2. In what follows, this model is referred to as the *discrete model*. The appropriate grid size is discussed in Appendix A where the two magnetic field models are compared. We select a sufficiently small grid spacing in the discrete model, and a sufficiently large maximum wave number $k_{\max}$ in the continuum model, to ensure that the magnetic field is fully resolved at the Larmor radius scale.

There are a few important subtleties in the numerical implementation of random magnetic fields on a mesh (i.e. in the discrete model), arising from the requirements of isotropy and randomness of phases (to a given accuracy). To ensure these at the outer scale k_0, there should be a sufficiently large number of modes at this wave number. In other words, there should be a sufficiently large sphere of (approximately) this radius in k-space. Failing to do this may affect the particle diffusion significantly. Therefore, the size of the computational domain in k-space should be larger than $k_{\max}/k_0$, and, correspondingly, the domain in physical space should be larger than $L = 2\pi/k_0$. If the isotropy and the randomness of phases have been achieved at the outer scale, smaller scales do not represent a problem in this respect. In addition to magnetic modes at the resonant wave number $k \approx 2\pi/R_{\mathrm{L}}$, previous studies have shown that the density of nearby wave numbers can be important for effective particle scattering with some types of magnetic field (e.g., Mace et al. 2012). Similar consideration may be important for both of our magnetic field constructions. We carefully test our numerical implementations of the magnetic field for isotropy at all relevant scales including $2\pi/k_0$ to ensure that the modes of a given wave number have randomly distributed phases. It seems that taking a mesh size $N_x = N_y = N_z \geq 4k_{\max}/k_0$ is sufficient if $k_{\max}$ is set to be the radius of the largest sphere that fits within the wave number domain. Larger mesh sizes may be preferable when $R_{\mathrm{L}} \gtrsim L$, but in that case one might compensate by reducing $k_{\max}/k_0$, since the small scales should have little influence on the particle transport (Plotnikov et al. 2011).

We use a trilinear interpolation from the nearest grid points to obtain the magnetic field between them. On one server with 256 GB of RAM we could achieve a resolution of up to 2048^3 mesh points. Larger resolutions, involving a mesh distributed in memory across multiple compute nodes, are much more computationally expensive and are not likely to provide any additional benefit in the present study. A magnetic field realization can be computed in much less than a minute of CPU time at a resolution 1024^3. It is desirable to use a large number of the magnetic field realisations, with as few particles per realisation as possible. For example, at 1024^3 around 30 realizations, each with about 50–100 particles can be performed within a reasonable time. However, in such a time, more particles per realisation have to be used as the mesh size increases in order to obtain sufficient statistics. Once the magnetic field has been computed, solving the particle equations of motion is relatively quick.

When magnetic field is defined using Equation (9) (i.e. in the continuum model), very little computer memory is needed because the field is computed only at the location of a particle. In this case, the number of modes N is limited by the computer time available because the field is computed repeatedly at each time step when the equations of motion are solved.

2.2 Equations of test particle motion

The position $\boldsymbol{x}$ of an energetic charged particle in magnetic field $\boldsymbol{B}$ is governed by the Newton–Lorentz equations,

$$\frac{d\boldsymbol{x}}{dt} = \boldsymbol{v}\,, \qquad \frac{d\boldsymbol{v}}{dt} = \frac{q}{\gamma mc}\boldsymbol{v} \times \boldsymbol{B}\,, \tag{13}$$

where $\boldsymbol{v}$ is the particle velocity, q and m are the particle charge and rest mass, $\gamma = 1/\sqrt{1 - v^2/c^2}$ is the Lorentz factor, $v = |\boldsymbol{v}|$, and c is the speed of light. Since the electric field has been neglected, particle energy is conserved. It is useful to define dimensionless variables

$$\boldsymbol{x}' = \frac{\boldsymbol{x}}{L}\,, \quad \boldsymbol{v}' = \frac{\boldsymbol{v}}{v_0}\,, \quad \boldsymbol{B}' = \frac{\boldsymbol{B}}{\mathcal{B}_0}\,, \quad t' = \frac{t}{t_0}\,,$$

with $t_0 = L/v_0$ and $\mathcal{B}_0 = (B_0^2 + b_0^2)^{1/2}$, in terms of L and an appropriate reference speed v_0; for relativistic particles, $v_0 \approx c$ is an appropriate choice. The resulting dimensionless form of Equations (13) is given by

$$\frac{d\boldsymbol{x}'}{dt'} = \boldsymbol{v}'\,, \qquad \frac{d\boldsymbol{v}'}{dt'} = \alpha\boldsymbol{v}' \times \boldsymbol{B}'\,, \tag{14}$$

where

$$\alpha = \frac{qL\mathcal{B}_0}{\gamma mcv_0}\,. \tag{15}$$

In this work we examine how the particle transport depends on the characteristic Larmor radius,

$$R_{\mathrm{L}} = \frac{\gamma mvc}{|q|\mathcal{B}_0} = \frac{pc}{|q|\mathcal{B}_0} = \frac{pc}{|q|}\frac{\sqrt{\eta}}{b_0}\,, \tag{16}$$

where $p = \gamma mv$ is the particle momentum. We note for the sake of the reader's convenience that R_{L} is related to the particle kinetic energy via $E_k = \sqrt{(R_{\mathrm{L}}q\mathcal{B}_0)^2 + m^2c^4} - mc^2$, or $E_k \propto R_{\mathrm{L}}$ for relativistic protons in a microgauss-strength magnetic field. The dimensionless Larmor radius is given by

$$R'_{\mathrm{L}} = R_{\mathrm{L}}/L = v'/\alpha\,.$$

We note that the Larmor radius is defined here with respect to the total rather than mean magnetic field strength.

Individual particles have random initial positions within a cube of approximate length L, the outer scale of the turbulence. The particle velocity is given a random initial direction with $|\boldsymbol{v}'| = 1$. We then solve equations of motion numerically for $\mathcal{B}'_0 = 1$ and set $R'_{\mathrm{L}} = \alpha^{-1}$ by selecting α as desired.

We solve Equations (14) numerically, primarily using the fifth-order method of Cash & Karp (1990), which allows for an adaptive

step size via the error estimate of the fourth-order solution. Additionally, in order to check if precise energy conservation is essential, we have sometimes used the highly conservative method of Boris (1970), which is widely used in particle-in-cell (PIC) plasma simulations. We find no appreciable difference in results between the two methods; however, the former is more efficient. Over all results reported here, the maximum particle kinetic energy change over the diffusion time $t_{\max}$ – which is typically $(10^1$–$10^2)t_0$, as is seen in Figure A1 – is around 0.1 per cent (but is often much less).

2.3 Diffusion coefficients

Time-dependent diffusion coefficients were obtained from test particle simulations using

$$\kappa_{xx}(t) = \frac{1}{2}\frac{\mathrm{d}}{\mathrm{d}t}\langle(\Delta x)^2\rangle = \langle v_x(t)\Delta x\rangle\,, \tag{17}$$

where Δx is the particle displacement in the x-direction over some time t, and $v_x(t)$ is the x-component of the particle velocity at the end of the displacement. The angular brackets in Equation (17) denote averaging over displacements for multiple time intervals of length t on a specific particle trajectory, over many particles and several (ideally, equally many) magnetic field realisations. Similar expressions were used to evaluate $\kappa_{yy}(t)$ and $\kappa_{zz}(t)$. In this work we are mainly interested in the asymptotic limit, $\kappa_{ij} = \lim_{t\to\infty}\kappa_{ij}(t)$, which can be approximated by taking $\kappa_{ij}(t)$ at a suitably large time. In this limit, Equation (17) is equivalent to

$$\kappa_{xx} = \lim_{t\to\infty}\frac{\langle(\Delta x)^2\rangle}{2t}, \tag{18}$$

which has been employed in other works (Section 1.3.1 of Shalchi 2009, and references therein). As illustrated and discussed in Appendix A, the two prescriptions are equivalent but the former is more convenient in simulations, especially when the time dependence of the diffusivity is as smooth and simple as in our case. In particular, the asymptotic diffusion coefficients are obtained from Equation (17) at an earlier computational time than with Equation (18).

Here we have no real interest in the off-diagonal elements κ_{ij}, where $i \neq j$, since they describe systematic drifts of cosmic-ray particles that are not likely to affect their large-scale diffusion (Section 1.6 of Shalchi 2009). We use the difference between the numerically obtained $\kappa_{xx}(t)$ and $\kappa_{yy}(t)$ as an estimate of the error in the diffusion coefficients; typically we obtain sufficient statistics to have the maximum running difference of less than three per cent. Note that for the diagonal elements of κ_{ij} — but not, in general, for the off-diagonal ones (Shalchi 2011) — the above relations produce the same result as the standard Taylor–Green–Kubo formula (Taylor 1922; Green 1951; Kubo 1957)

$$\kappa_{ij}(t) = \int_0^\infty \langle v_i(0)v_j(t)\rangle dt, \tag{19}$$

where $v_i(t)$ is the velocity component in the direction x_i at time t.

The diffusion coefficients κ_{ij} thus obtained are related, via a relation similar to Equation (2), to the diffusivities $\kappa_\perp$ and $\kappa_\parallel$ across and along the magnetic field at the largest scale available, which is comparable to L in our implementations of the random magnetic field. In contrast, the parallel and perpendicular diffusivities $K_\parallel$ and $K_\perp$ of Equation (2) are defined with respect to $\boldsymbol{B}_0$, the magnetic field averaged over scales larger than the turbulent ones. Therefore, we call κ_{ij}, $\kappa_\parallel$ and $\kappa_\perp$ the *local* diffusivities. In the context of sub-grid modelling of cosmic ray diffusion, the scale L is close to the smallest resolved scale in an MHD simulation, and the effects of magnetic fields at larger scales, approximated by Equation (2), should be faithfully reproduced by the cosmic-ray propagation equation with only the resolved magnetic field, using the diffusion tensor κ_{ij}.

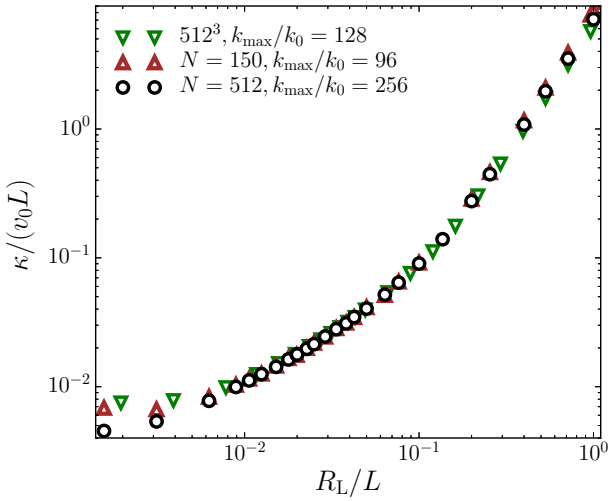

Figure 1. Different implementations of a purely random magnetic field (with $s = 5/3$) lead to consistent values of the isotropic diffusivity for $R_{\rm L}/l_{\rm c} \ll 1$ (with $l_{\rm c} \approx 0.1L$). Circles and upward triangles are for the continuous model, and downward triangles are for the discrete model. For $R_{\rm L} > l_{\rm c}$, the diffusivity scales as $R_{\rm L}^2$, but the results from the different magnetic field models diverge with increasing $R_{\rm L}$ for the reasons discussed in Appendix A. For $s = 3/2$, similar trends are observed.

The continuum and discrete magnetic field models are compared in Appendix A where we present the running diffusion coefficient obtained for a various values of $R_{\rm L}/l_{\rm c}$ and numerical resolutions. The range of variation in the values of the diffusivity, obtained under widely varying numerical resolutions (512^3–1536^3) in model (12), and number of modes ($N = 150$–1024) in model (9), decreases from less than 20 per cent for $R_{\rm L}/l_{\rm c} = 5$ to about 5 per cent for $R_{\rm L}/l_{\rm c} \leq 1$. Based on these tests, we initially decided to use $N = 150$ and $k_{\max}/k_0 = 96$ with the continuous model (9) and the resolution 512^3 with $k_{\max}/k_0 = 128$ with the discrete model (12).

3 DIFFUSION IN A PURELY RANDOM MAGNETIC FIELD

Figure 1 shows the asymptotic (in time) isotropic diffusion coefficient κ_0 as a function of $R_{\rm L}/L$ for $s = 5/3$ and $\eta = 1$ (zero mean field) obtained with various magnetic field models and resolutions. A linear scaling at $R_{\rm L} \ll l_{\rm c}$ and a quadratic scaling at $R_{\rm L} \gg l_{\rm c}$ are found. The latter scaling is consistent with both theory and earlier test particle simulations (see Parizot 2004; Plotnikov et al. 2011, and references therein). However, the differences between the diffusivities obtained with different magnetic field models increase with $R_{\rm L}/L$ for a *fixed* resolution and $k_{\max}/k_0$. As discussed in Appendix A, this can be remedied by changing the range, number density and/or location of the magnetic modes in k-space.

On the other hand, results at $R_{\rm L} \ll l_{\rm c}$ exhibit an encouragingly weak dependence on the details of the magnetic field model. Figure 2 illustrates this regime in finer detail where we have added

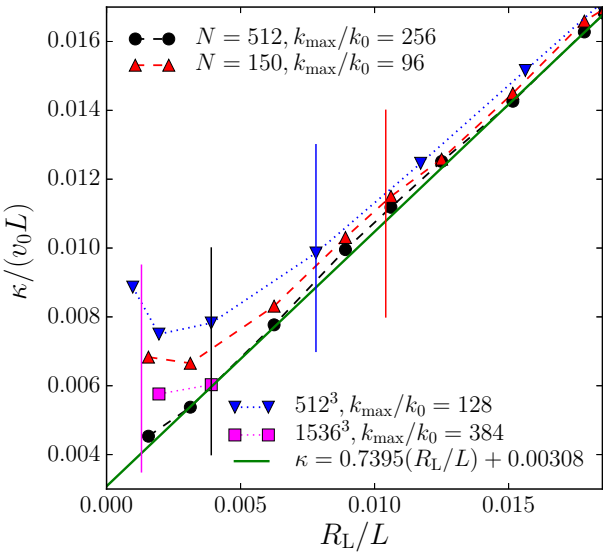

Figure 2. The isotropic diffusion coefficient κ_0 at $R_{\rm L} \ll l_{\rm c} \approx 0.1L$ for $\eta = 1$ and $s = 5/3$ with the best fit to the most highly-resolved data shown with (green) solid line (see the text and Figure 3). The linear dependence of κ_0 on $R_{\rm L}$ extends to very small values of $R_{\rm L}$, provided $k_{\max}/k_0$ is large enough. The vertical lines of the corresponding colour indicate $R_{\rm L} = 2\pi/k_{\max}$ for the various parameter values used. The numerical resolutions, mode numbers and magnetic field models used are specified in the legend. Deviations from the asymptotic linear dependence of κ_0 on $R_{\rm L}/L$ at small values of this ratio are sensitive to these factors.

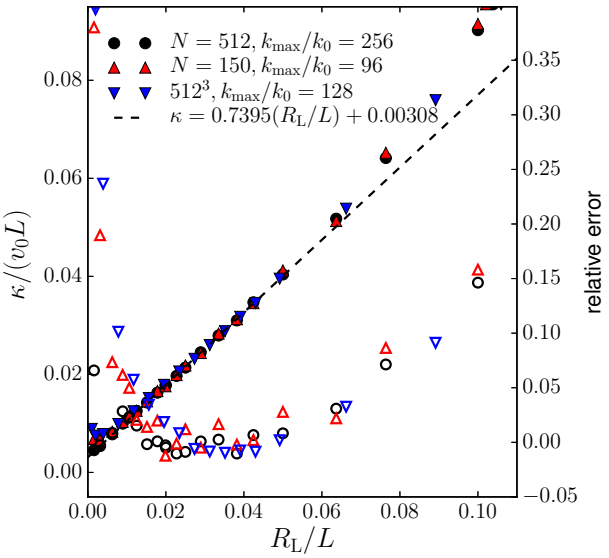

Figure 3. The isotropic diffusivity κ_0 at low $R_{\rm L}$ in a continuous and discrete random magnetic fields with the number of modes N, $k_{\max}/k_0$ and the resolution specified in the legend. The best fit of Equation (20) is shown with dashed line (also shown solid in Figure 2). Open symbols show the corresponding relative deviations from the best fit (the right-hand ordinate axis).

additional results from a discrete magnetic field model at a resolution 1536^3 with $k_{\max}$ three times larger than that with the 512^3 resolution. In the 512^3 case, deviations from the linear trend shown by the solid line line start almost from the extreme right of the range of $R_{\rm L}$ shown. The solid blue vertical line (the second vertical line from the right) shows where $R_{\rm L} = 2\pi/k_{\max}$, i.e. at the scale of the smallest structures in the magnetic field; significant deviations from the linear trend occur below this marker. With the 1536^3 grid, deviations from the straight line are much weaker (the leftmost vertical line marks $R_{\rm L} = 2\pi/k_{\max}$ for this case). With the continuum magnetic field model, the deviation from the linear trend is weaker than that in the case of a discrete model with a similar value of $k_{\max}$. These results seem to indicate that the continuation of the linear trend down to smaller $R_{\rm L}$ depends on the presence of magnetic modes at or near to the resonant wave number $k_{\rm res} = 2\pi/R_{\rm L}$. Suppression of such modes presumably leads to an increased particle mean free path parallel to the local magnetic field, resulting in an enhanced diffusion coefficient, as observed in Figure 2. Given that the continuum model has very few modes at large k, it is perhaps surprising that deviation from the linear trend occurs at approximately $R_{\rm L} = 2\pi/k_{\max}$, whereas the discrete magnetic field model, containing many more modes near that scale, deviates from the linear trend at a somewhat higher value of $R_{\rm L}$. One reason for this can be that the high-k modes in the discrete model are not sufficiently well resolved in k-space. It may also be the case that the numerical construction curtails energy at the smallest scales. Furthermore, at these extremes $R_{\rm L}$ is close to the grid resolution on which the magnetic field is defined, and errors from the trilinear interpolation between mesh points can have some effect. These results suggest that caution is required, and that $R_{\rm L}$ should not be less than about three separations of the mesh on which magnetic field is defined.

Simulations for still smaller values of $R_{\rm L}/L$ are more computationally efficient with the continuous magnetic field model. We explored the range down to $R_{\rm L}/L = 10^{-3}$ using up to $N = 5000$ modes; the diffusion coefficient remains very close to the solid line shown in Figure 2. Casse et al. (2001) found a Bohm scaling of the diffusion coefficient, $\kappa \propto R_{\rm L} v_0$, similar to our results in a limited range of $R_{\rm L}$. However, these authors find a different scaling below a certain value of $R_{\rm L}$ (see also Fatuzzo et al. 2010). It is not clear why the result found here is different from those; the most obvious difference is that those simulations used $k_{\max}/k_0 = 10^4$ with only $N = 200$ modes in their continuous magnetic field model. Here we confirm the linear scaling of κ_0 with $R_{\rm L}/l_{\rm c}$ down to very small values of $R_{\rm L}/l_{\rm c}$ with both magnetic field implementations.

In Figure 3 we show a fit of the form

$$\frac{\kappa_0(R_{\rm L})}{v_0 L} \approx 0.0031 + 0.74\,\frac{R_{\rm L}}{L} \qquad (20)$$

to the isotropic diffusivity obtained with $k_{\max}/k_0 = 256$ over the range where the variation with $R_{\rm L}/L$ is linear, $4 \times 10^{-3} \lesssim R_{\rm L}/L \lesssim 5 \times 10^{-2}$ with $l_{\rm c} \approx 0.1$. The relative deviations from the fit are shown in Figure 1; they do not exceed about 15 per cent at $R_{\rm L} = l_{\rm c}$ (i.e., $R_{\rm L}/L \approx 0.1$), where we might have expected more deviation, given the tendency towards quadratic scaling with $R_{\rm L}$ at around $R_{\rm L} = l_{\rm c}$. The fit approximates the numerical results to within 3 per cent for all values of $R_{\rm L}$, between $R_{\rm L} = l_{\rm c}/2$ and the smallest values of $R_{\rm L}$ considered (where already $R_{\rm L} < 2\pi/k_{\max}$, resulting in reduced resonant scattering).

The fit has a non-zero intercept,

$$\kappa_0|_{R_{\rm L}\to 0} \approx 3 \times 10^{-3} v_0 L\,, \qquad (21)$$

corresponding to a part of the diffusivity independent of the Larmor radius (i.e., the particle energy). For $v_0 = c$, and $L \simeq 100\,{\rm pc}$ for the outer turbulent scale, we obtain $\kappa_0 \simeq 3 \times 10^{28}\,{\rm cm}^2\,s^{-1}$. We can compare this result to an estimate based on the particle diffusion along random magnetic lines (Jokipii & Parker 1968), known

as the field line random walk (FLRW) model. If particles are tied to the magnetic lines and maintain a constant pitch angle, the diffusion coefficient perpendicular to the magnetic field can be estimated as the magnetic field line diffusion coefficient (defined as the spatial divergence rate of the magnetic lines – see below) multiplied by the particle velocity parallel to the field lines, i.e., $\kappa = \tilde{v}D_b/3$, where D_b is the magnetic field line diffusion coefficient, as defined below, and $\tilde{v}/3$ is the characteristic particle speed along the field line, with the factor $1/3$ being appropriate for the isotropic case. Note that it is more intuitive to make such a calculation when $\eta \ll 1$, where the diffusion coefficient is essentially measured perpendicular to the mean magnetic field line; nevertheless, here we will associate κ with perpendicular diffusion, although there is no preferred direction in the isotropic case $\eta = 1$. Let us now define D_b for a general η, since it will be useful in subsequent sections where $\eta < 1$. Consider random magnetic field line displacements Δx_i^{FL} as a function of the arc length s, measured along the magnetic line (i.e. the change in field line position with s). Then defining

$$D_{b,i} = \tfrac{1}{2} \lim_{s\to\infty} \frac{\mathrm{d}\langle(\Delta x_i^{\mathrm{FL}})^2\rangle}{\mathrm{d}s}\,, \tag{22}$$

we take $D_b = \frac{1}{3}\sum_{i=1}^{3} D_{b,i}$ for $\eta = 1$ and $D_b = \frac{1}{2}\sum_{i=1}^{2} D_{b,i}$ when $\eta < 1$ and $\boldsymbol{B}_0 \parallel \widehat{\boldsymbol{x}}_3$. Note that D_b has the dimension of length. We evaluate Equation (22) numerically by solving field line equations for many field lines over several magnetic field realisations, essentially as described by Sonsrettee et al. (2015b). Alternatively, Sonsrettee et al. (2015b) provide an analytical approximation of D_b in terms of l_{c} or another length scale from the magnetic power spectrum. In both cases, for $\eta = 1$ we find that $D_b \approx 0.06L$. Due to the pitch angle scattering, particles travel back and forth along magnetic lines, so that $\tilde{v}$ can be much smaller than the instantaneous particle speed v_0. Equation (21) is obtained for $\tilde{v} \approx 0.15v_0$. If this model is correct, then the parallel scattering would have to be non-diffusive, otherwise we would obtain compound subdiffusion (Urch 1977; Kóta & Jokipii 2000) perpendicular to the magnetic lines. A more likely scenario is that particles eventually escape to nearby field lines, so that the FLRW limit is invalid.

To gain further insight into the nature of Equation (20), we considered various forms of the magnetic power spectrum $M(k)$. When its slope is $s = 3/2$, rather than $s = 5/3$, we have

$$\frac{\kappa_0(R_{\mathrm{L}})}{v_0 L} \approx 0.0019 + 0.76\,\frac{R_{\mathrm{L}}}{L}\,,$$

that is, a similar slope with the intercept different by 30 per cent from that in Equation (20). We also considered magnetic spectrum of the form (8) with $s = 5/3$ and $k_b = 5k_0$ to obtain

$$\frac{\kappa_0(R_{\mathrm{L}})}{v_0 L} \approx 0.0017 + 0.75\,\frac{R_{\mathrm{L}}}{L}\,,$$

which, again, is similar to the other two forms but with yet another value for the intercept, about a half of that obtained for $s = 5/3$. This suggests that $\kappa_0|_{R_{\mathrm{L}}\to 0}$ depends on the form of the magnetic power spectrum, but that this dependence is not very strong, variations remaining within a factor of two for reasonable forms of the spectrum.

4 DIFFUSION IN A PARTIALLY ORDERED MAGNETIC FIELD

In this section we consider cosmic ray diffusion in a magnetic field with $\eta < 1$, where $\boldsymbol{B}_0$ is aligned with the z-axis ($z \equiv x_3$).

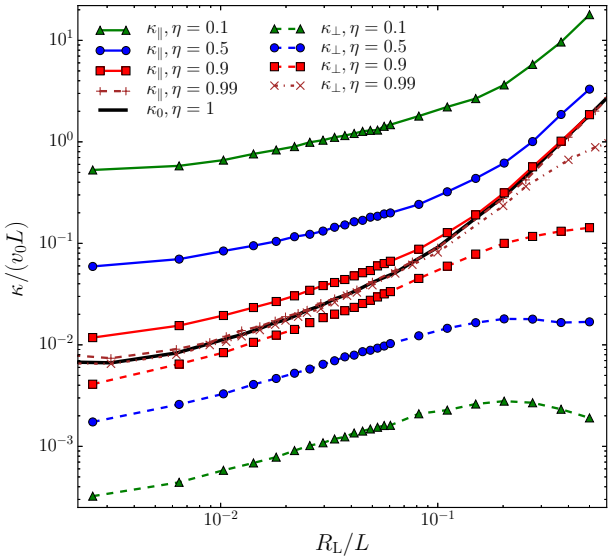

Figure 4. Asymptotic (in time) diffusion coefficients $\kappa_\perp$ and $\kappa_\parallel$, for various values of η specified in the legend, as functions of R_{L} for the continuous magnetic field model with $s = 5/3$ and $k_{\max}/k_0 = 200$. The black solid curve shows the diffusivity in the corresponding purely random magnetic field as in Section 3.

Figure 4 shows the *local* parallel and perpendicular diffusion coefficients $\kappa_\parallel$ and $\kappa_\perp$ for several values of η as a function of R_{L}, for the magnetic spectrum (6) with $s = 5/3$. A reduction in the pitch angle scattering is expected where $R_{\mathrm{L}} < 2\pi/k_{\max}$, that is $R_{\mathrm{L}}/L < k_0/k_{\max} = 5 \times 10^{-3}$ (the latter equality applies for the parameter values used in Figure 4). This is evidenced in the deviation from the trend of the diffusion coefficients at the smallest values of R_{L}/L plotted in the figure. Although this is not easy to see in the figure itself, the behaviour is similar to that seen in Figure 2 when plotted on a linear scale. For a given R_{L}, the diffusivity in a purely random magnetic field, κ_0 obtained at $\eta = 1$, separates regions in Figure 4 filled with the curves representing $\kappa_\parallel$ in the upper part and $\kappa_\perp$ in the lower: $\kappa_\perp < \kappa_0 < \kappa_\parallel$.

Before considering the range $R_{\mathrm{L}}/L \ll 1$, our main concern here, a few comments on the region of larger values of R_{L}, where $R_{\mathrm{L}}/L \geq l_{\mathrm{c}}/L = 0.1$ might be appropriate. Here $\kappa_\parallel \propto R_{\mathrm{L}}^2$, while $\kappa_\perp$ tends to become independent of R_{L}/L. Plotnikov et al. (2011) explored the range $\eta \geq 0.5$ to find that $\kappa_\perp/\kappa_\parallel \propto R_{\mathrm{L}}^{-2}$ at large R_{L}, even when η is very close to unity (which implies a significant reduction of $\kappa_\perp$ from κ_0 for any $B_0 > 0$). Our results reproduce this behaviour for $\eta = 0.5$, but we have not explored large enough R_{L} to observe it at larger values of η. However, $\kappa_\perp$ decreases with increasing R_{L} for $\eta = 0.1$ and 0.5, rather than becoming independent of R_{L}/L. In the rest of this section we consider small R_{L}.

4.1 Parallel diffusion

For a given R_{L}, we find that $\kappa_\parallel$ scales quadratically with B_0/b_0 — or linearly with $(1-\eta)/\eta$ — as shown in Figure 5. The numerical results can be represented by κ_0 of Equation (20) with the addition of a slowly varying power law function of R_{L}, of the form aR_{L}^b. We fitted the two parameters a and b at small values of R_{L} to obtain the following approximation shown in Figure 5 with dashed lines:

$$\frac{\kappa_\parallel(R_{\mathrm{L}},\eta)}{v_0 L} \approx \frac{\kappa_0(R_{\mathrm{L}})}{v_0 L} + \tfrac{1}{3}\left(\frac{R_{\mathrm{L}}}{L}\right)^{1/3}\frac{1-\eta}{\eta}\,. \tag{23}$$

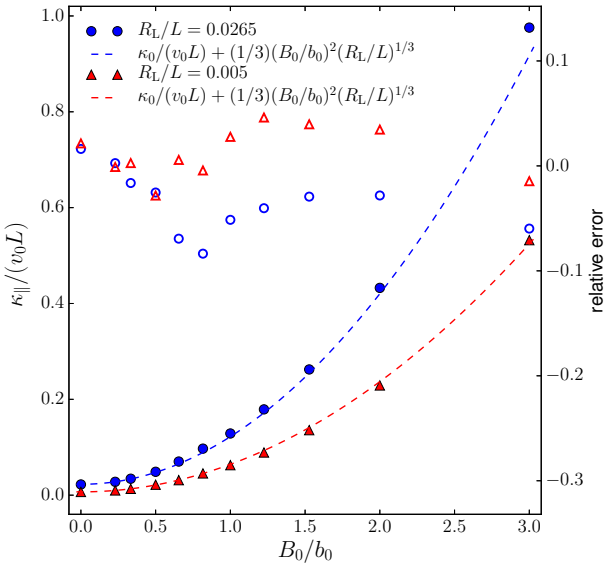

Figure 5. The local parallel diffusivity $\kappa_\parallel$ plotted versus $B_0/b_0 = \sqrt{(1-\eta)/\eta}$ for two values of R_L, together with their approximations (see the text). Filled (blue) circles are for $R_\mathrm{L} = l_\mathrm{c}/4$, where the relative error in the approximation is less than 10 per cent for the range of B_0/b_0 shown ($0.1 \leq \eta \leq 1$) (as shown by open circles, with the axis on the right of the frame). For the smaller value $R_\mathrm{L}/L = 0.005$ (filled triangles), the error (open triangles) is still smaller at a few per cent.

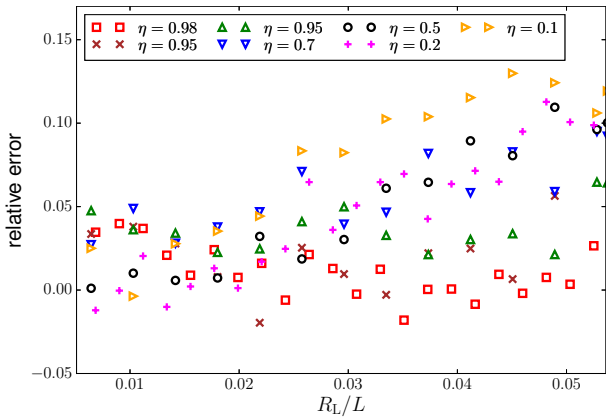

Figure 6. The relative error in the approximation for $\kappa_\parallel$ given by Equation (23) to the test particle simulations for various values of η given in the legend. The largest values of R_L shown correspond to $R_\mathrm{L} \approx l_\mathrm{c}/2$.

We note that the final term has the same scaling as is obtained from quasilinear theory (Jokipii 1966). In particular, for the magnetic spectrum (6), and assuming magnetohydrodynamic waves propagating parallel to the mean field, the appropriate quasilinear result is (e.g., Berezinskii et al. 1990; Schlickeiser 2002, and references therein)

$$\kappa_\parallel^{\mathrm{Q}L} = \frac{4v_0 L\,(2\pi)^{-s}}{(s-1)(2-s)(4-s)} \left(\frac{B_0}{b_0}\right)^2 \left(\frac{R_\mathrm{L}}{L}\right)^{2-s}, \tag{24}$$

which for $s = 5/3$ gives

$$\frac{\kappa_\parallel^{\mathrm{Q}L}}{v_0 L} \approx 0.36 \left(\frac{R_\mathrm{L}}{L}\right)^{1/3} \frac{1-\eta}{\eta}, \tag{25}$$

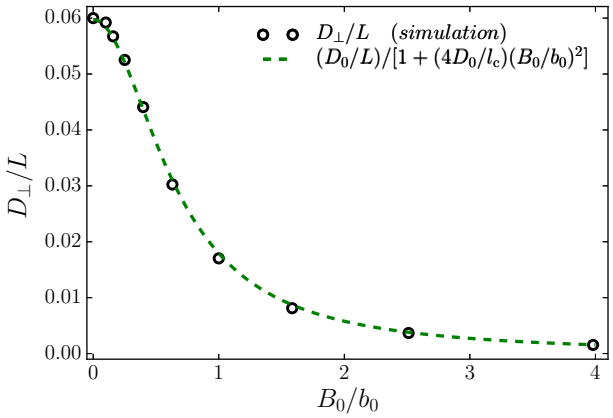

Figure 7. Perpendicular magnetic field line diffusion coefficients from test field line simulations as a function of B_0/b_0 and a theoretically motivated approximation (see text) for $s = 5/3$. Here $D_0 = D_\perp|_{B_0=0}$. Note that the factor $4D_0/l_\mathrm{c} \approx 2.4$, obtained here analytically, is not expected to depend strongly on s.

which is in very good agreement with the fitted term above. For $s = 3/2$ and $\eta = 0.5$ a fit to the data yields a similar scaling. An important point to note is that the usual definition of R_L in Equation (24) (i.e., with respect to the mean field) deviates from our definition in the limit $\eta \to 1$. Figure 6 demonstrates the fair quality of approximation of the test particle simulations for various η and R_L. For $R_\mathrm{L} \leq l_\mathrm{c}/4 \approx 0.025L$, the accuracy is better than five per cent, and within 10 per cent at $R_\mathrm{L} = l_\mathrm{c}/2$.

4.2 Perpendicular diffusion for $R_\mathrm{L} \ll l_\mathrm{c}$

We find that for the local perpendicular diffusivity obtained in our simulations, the expression

$$\kappa_\perp(R_\mathrm{L}, \eta) = \frac{\kappa_0(R_\mathrm{L})}{1 + \chi(B_0/b_0)^2} \tag{26}$$

provides a good approximation when $R_\mathrm{L} \ll l_\mathrm{c}$. Here χ is a constant around 2 or 3 that is not very sensitive to the value of R_L and $\kappa_0(R_\mathrm{L})$ is given by Equation (20). We have arrived at this form by first comparing the magnetic field line diffusion coefficient D_b, as discussed in Section 3, with $\kappa_\perp$, motivated by previous test particle simulations (e.g., Michalek & Ostrowski 1997; Ruffolo et al. 2008) that have shown that these two quantities are related. We calculated D_b for various values of B_0/b_0 using test magnetic line simulations and compared this with $\kappa_\perp$ from our test particle simulations. For a given R_L, our results show approximately $\kappa_\perp \propto D_b$ for a large range of B_0/b_0. Then using Equation (20) we can write

$$\kappa_\perp(R_\mathrm{L}, \eta) = \kappa_0(R_\mathrm{L}) D_b(\eta)/D_0, \tag{27}$$

where $D_0 = D_b|_{B_0=0}$. As mentioned in Section 3, D_0 can be approximated analytically in units of l_c (Sonsrettee et al. 2015b). We have no general expression for D_b, but Sonsrettee et al. (2015a) have derived analytical expressions in the limit $B_0/b_0 \to \infty$ and shown that a simple rational function which interpolates between D_0 and this limit describes test field line simulations very well. Following these authors, for large B_0/b_0 we have $D_b \to D_\infty = (l_\mathrm{c}/4)(b_0/B_0)^2$, then we obtain the expression

$$D_b(\eta) \approx \frac{D_0}{1 + D_0/D_\infty} = \frac{D_0}{1 + (4D_0/l_\mathrm{c})(B_0/b_0)^2}, \tag{28}$$

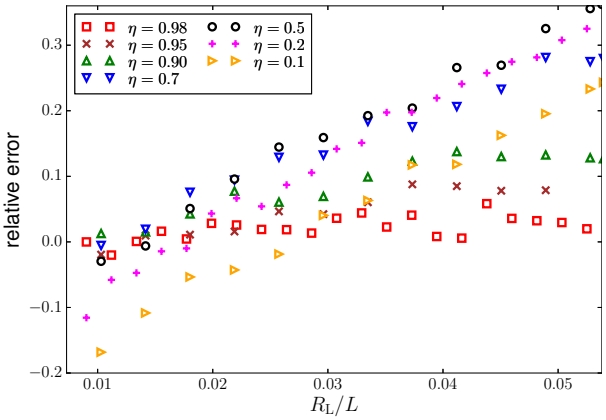

Figure 8. The relative error in the fit given by Equation (26) (using $\chi = 2.35$) to $\kappa_\perp$ obtained from test particle simulations shown for various values of R_L and η. The smallest R_L is at the scale $2\pi/k_\mathrm{max}$ and the largest at $l_\mathrm{c}/2$. Although the errors are quite small, they vary systematically with R_L/L, suggesting that there is a missing further dependence on R_L.

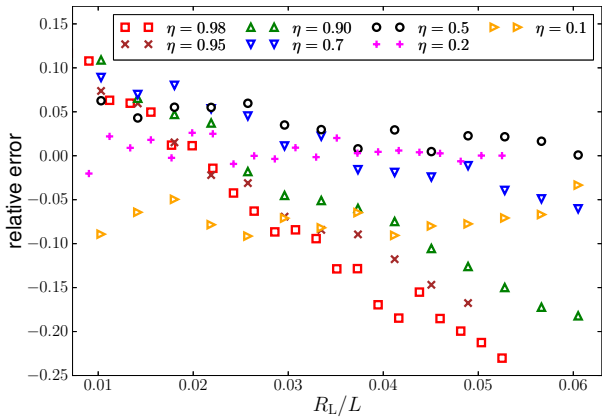

Figure 9. As Figure 8, but with the approximate form of $\kappa_\perp$ given by Equation (29).

where we have introduced a rational function that interpolates between D_0 and D_∞. As shown in Figure 7, this is in very good agreement with our test field line simulations. Finally, substituting Equation (28) into Equation (27), we obtain Equation (26) with $\chi = 4D_0/l_\mathrm{c}$. If we take D_0 obtained directly from field line simulations we get $\chi \approx 2.35$, which is very close to the theoretical value $\chi = 2.4$ used in Figure 7.

We also obtained D_0 from simulation using $s = 3/2$; for these, $\chi \approx 2.44$, which only differs from the $s = 5/3$ value by a few per cent, which is about the same size as the error. Moreover, since there are reasonable arguments that D_0 should scale linearly with l_c, we expect that χ should be essentially a constant, independent of the detailed form of the magnetic spectrum.

In the following subsection we compare Equation (26) and some improvements directly with our test particle simulation data.

4.3 Perpendicular diffusion for $R_\mathrm{L} \lesssim l_\mathrm{c}/2$

As shown in Figure 8, $\chi = 4D_0/l_\mathrm{c}$ in Equation (26) provides a very good approximation to $\kappa_\perp$ obtained from test particle simulations. However modest in magnitude, the relative error varies

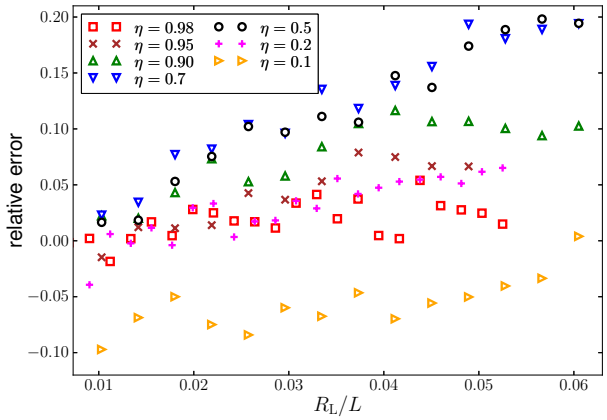

Figure 10. As Figure 8, but with the $\kappa_\perp$ given by Equation (30).

systematically with R_L, inviting a more accurate approximation. Figure 8 suggests an additional power-law factor in R_L with the exponent of 0.54–0.72 for a given η. For $\eta = 0.2$, we fitted the numerical results in the range $0 \le R_\mathrm{L} \le l_\mathrm{c}$ to obtain

$$\frac{\kappa_\perp(R_\mathrm{L},\eta)}{v_0 L} \approx \frac{0.19(R_\mathrm{L}/L)^{0.61}}{1 + (4D_0/l_\mathrm{c})[\,(1-\eta)/\eta\,]}\,, \tag{29}$$

where the exponent has a standard error of less than one per cent. For $\eta = 0.5$, the numerator becomes $0.20(R_\mathrm{L}/L)^{0.64}$, with a similarly small error. Furthermore, the numerator exhibits a dependence on η. The relative difference between the fit at $\eta = 0.2$ and the numerical results at different values of η is shown in Figure 9. For $\eta \to 1$, the difference varies linearly with R_L/L, similarly to κ_0 in Equation (20) or the related approximations of Section 3. However, variation with a smaller exponent is apparent when $\eta \to 0$. The following heuristic form with a linear transition between these regimes appears to be a suitable improvement of Equation (29):

$$\frac{\kappa_\perp(R_\mathrm{L},\eta)}{v_0 L} \approx \frac{\eta\dfrac{\kappa_0}{v_0 L} + 0.19\,(1-\eta)\left(\dfrac{R_\mathrm{L}}{L}\right)^{0.61}}{1 + \dfrac{4D_0}{l_\mathrm{c}}\,\dfrac{1-\eta}{\eta}}\,. \tag{30}$$

The deviations of the numerical results from this form are shown in Figure 10.

5 SUMMARY AND DISCUSSION

The main outcome of our work is a set of approximate expressions for the diffusion tensor that apply to cosmic ray propagation in a random magnetic field that has sufficient energy at the Larmor radius scale to scatter the particles. The latter condition is not a generic constraint but rather a result of the limitations of the model (for example, our model magnetic field does not include the propagation of magnetohydrodynamic waves, which should relax this constraint in a physical manner). Our results can be represented as combinations of existing theoretical ideas and analytical estimates, in forms which may have been difficult to envisage without detailed computations.

Our main motivation has been to make a first step towards a sub-grid model of cosmic ray propagation in the MHD context, that captures the dependence of the cosmic ray diffusion on the local physical parameters of the plasma. We envisage that the approximations to the elements of the diffusion tensor derived here

may be used with the values of η and L obtained from the magnetic field parameters near the smallest resolved scales of an MHD simulation. It is presumed that the effects of the magnetic field at scales larger than the numerical resolution would be accounted for by the solution of equations for cosmic-ray dynamics, e.g., in the advection–diffusion approximation.

The main contribution to the large-scale dynamics of interstellar and intergalactic plasmas comes from cosmic ray particles in the GeV energy range whose Larmor radius $R_{\rm L}$ is by far smaller than any other scale in the MHD approximation. Therefore, a sub-grid model should be based on a description of the cosmic ray diffusion in the limit $R_{\rm L}/\delta x \ll 1$, where δx is the numerical resolution length. Most studies of cosmic ray diffusion are in the opposite limiting case, where the Larmor radius is comparable to or larger than the magnetic turbulent scale. Furthermore, calculations of the diffusion tensor K_{ij} are usually presented in a reference frame connected with the *global* mean magnetic field. In our case, such a mean magnetic field is undefined since there are no reasons to expect any scale separation in the magnetic fields at length scales of a few parsecs. Therefore, we present our results in terms of the *local* diffusivities κ_{ij} defined with respect to the local magnetic field.

We have found the following approximations to the elements of the diffusion cosmic ray tensor valid when the particles' Larmor radius is much smaller than the scale of magnetic turbulence, $R_{\rm L} \ll l_{\rm c}$, with $l_{\rm c}$ the correlation length; we defer comparison of the approximations with previous results till later in this section.

In a purely random magnetic field, fits to the simulation data in Section 3 suggest that the isotropic diffusivity can be approximated by

$$\kappa_0(R_{\rm L}) \approx v_0 L \left(a_1 + a_2 \frac{R_{\rm L}}{L}\right), \qquad (31)$$

where v_0 is the particle speed, L is the outer turbulence scale and the parameters a_1 and a_2 depend on the magnetic power spectrum. The factor a_2 changes more weakly with the spectrum than a_1, at least for the spectra explored. For a power-law spectrum with the exponent $s = 5/3$, we have obtained $a_1 \approx 3.1 \times 10^{-3}$ and $a_2 \approx 0.74$, compared to $a_1 \approx 1.9 \times 10^{-3}$ and $a_2 \approx 0.76$ for $s = 3/2$. These approximations remain accurate to within about 15 per cent up to $R_{\rm L} = l_{\rm c}$. For relativistic particles ($v_0 = c$) in a field of $5\,\mu$G with $L = 100\,$pc, these expressions imply a minimum parallel diffusion coefficient of (2–3) $\times\, 10^{28}\,{\rm cm}^2\,{\rm s}^{-1}$ (in the limit of a vanishing mean field, $\eta \to 1$).

In a partially ordered magnetic field, with the mean strength B_0 and the root-mean-square random part b_0, the parallel diffusivity of the form (23), approximates our numerical results for $0 < B_0/b_0 \leq 1/3$ to within about five per cent at $R_{\rm L} = l_{\rm c}/4$ (and better at smaller values of $R_{\rm L}$). The perpendicular diffusivity is approximated by Equation (26) with $\chi = 4D_0/l_{\rm c}$, where D_0 is the isotropic magnetic field line diffusion coefficient (related to the divergence of magnetic lines) of Equation (22) for $\eta = 1$, controlled by the integral length scale of the magnetic spectrum, $D_0/l_{\rm c} \approx 0.6$.

Although it is not our primary concern in this paper, we have obtained the following results for $R_{\rm L} \lesssim l_{\rm c}/2$. The perpendicular diffusion coefficient exhibits an $R_{\rm L}$-dependence which is not captured by the term containing κ_0 in Equation (26). For $R_{\rm L} \gtrsim 10^{-3} l_{\rm c}$, $\kappa_\perp$ might be better approximated by Equation (29). There is a further, weaker dependence on η, which can be allowed for using Equation (30). A still better approximation might have the constant χ in Equation (26) replaced by a function of $R_{\rm L}$ and/or η. Nevertheless, all the given expressions provide a very good approximation over the range of $R_{\rm L}$ considered.

To illustrate these results, consider an application to MHD simulations of the ISM adopting, as typical parameters, $B_0 = 2\,\mu$G, $b_0 = 5\,\mu$G, $L = 100\,$pc, $s = 5/3$ and $R_{\rm L} = 3.3 \times 10^{12}\,$cm. Recent extensive simulations of the supernova-driven ISM have the numerical resolution of order $\delta x \simeq 1\,$pc. The random magnetic field expected at this scale is of the order of $b|_{\delta x} \simeq b_0 (\delta x/L)^{1/3} \simeq 1\,\mu$G. Our intention is to estimate the effective diffusion coefficients at this scale. For this purpose we can adopt in our diffusion coefficient expressions, δx and $b|_{\delta x}$ as the outer scale and fluctuation strength, respectively. The η-dependent term in the expression for the parallel local diffusivity (23) is then of order 10^{-2} and is independent of δx. This is about three times larger than the value of $\kappa_0/(v_0 L)|_{L=\delta x}$ estimated in Section 3, and we find $\kappa_\parallel \approx 1.4 \times 10^{27}\,{\rm cm}^2\,{\rm s}^{-1}$. From Equation (26) we obtain $\kappa_\perp \approx 3 \times 10^{25}\,{\rm cm}^2\,{\rm s}^{-1}$, and $\kappa_\parallel/\kappa_\perp \approx 50$. The random walk of numerically resolved magnetic lines should lead to a more isotropic diffusion tensor and when applying the usual lengthscale L and fluctuation strength b_0 in our expressions we obtain $\kappa_\parallel/\kappa_\perp \approx 1.5$, which is in reasonable agreement with the expectation of isotropization at large scales (Berezinskii et al. 1990). Then the cosmic ray diffusivities approximated here can be usefully applied to such MHD simulations with b_0 obtained using the random magnetic field at the smallest numerically resolved scale.

There are other plausible interpretations of the estimated diffusivities. Cosmic ray diffusion is controlled at the resonant scales, and a more relevant value of b_0 to be used could be that at the Larmor radius scale. The random magnetic field extrapolated to the Larmor-radius scale, $b|_{R_{\rm L}} \simeq b_0 (R_{\rm L}/L)^{1/3} \simeq 4 \times 10^{-3}\,\mu$G, is very weak indeed. Since magnetic field at scales exceeding δx is fully resolved, its effect on cosmic ray diffusion does not need to be included into the sub-grid model of diffusion. Then in place of B_0, the appropriate effective mean magnetic field could be the root-mean-square field at the scale δx, $b_{\delta x} \simeq 1\,\mu$G. Taking these values, the $R_{\rm L}$-dependent term in the isotropic diffusivity (31) is negligible, whereas the η-dependent term in the expression for the parallel local diffusivity (23) is about 30. Using Equation (30), we then obtain $\kappa_\parallel/\kappa_\perp \simeq 10^7$. In this scenario, the cosmic ray diffusion tensor is highly anisotropic at small scales and cosmic rays are partially isotropized when propagating in the random magnetic field at scales exceeding $\delta x \simeq 1\,$pc. Further development and implementation of a sub-grid model for cosmic-ray diffusion will be discussed elsewhere.

The random magnetic field resolved in MHD simulations of the ISM would enhance cosmic ray diffusion through the random walk of magnetic lines, modelled faithfully by solving simultaneously the MHD and cosmic-ray equations with the diffusivity tensor dependent on the magnetic field direction. This process is expected to be more complicated than usually assumed, and perhaps very different from the predictions of existing models of cosmic ray propagation in random magnetic fields, because a significant part of the random magnetic field in the ISM is produced by compression in the shocks driven by supernova remnants, and by fluctuation dynamo action. Both processes produce random magnetic fields represented by widely separated, intense structures against a distributed background; such a random field is strongly intermittent. The structures associated with the magnetic intermittency are magnetic sheets and filaments, resulting from shock-wave compression and the fluctuation dynamo (Zeldovich et al. 1990; Beck et al. 1996; Wilkin et al. 2007), respectively. Interstellar random magnetic fields are expected to have a significant non-Gaussian part,

and the random-phase approximation, as employed here and in several other works, does not apply to such structures. The magnetic structures can affect the cosmic ray transport significantly by introducing Lévy flights of the particles, which would be trapped for a relatively long time within the structures and move more freely over larger distances between them. This picture also applies to intergalactic space where the fluctuation dynamo may be active (e.g., Akahori & Ryu 2011). The fractional volume of magnetic filaments produced in the ISM by the fluctuation dynamo is estimated to be of order 0.01–0.1 (Sect. 7.4.2 in Shukurov 2007). Fletcher & Shukurov (2007) estimate the mean separation between the supernova shocks in the ISM to be of the order of 10 pc and argue that polarization observations of the nearby ISM at low radio frequencies are consistent with this estimate. It is noteworthy that the localised magnetic structures have scales by far larger than either the relevant Larmor radii or the resolution of MHD simulations of the ISM. Therefore, magnetic field models that are free from intermittency, similar to those used here, are quite appropriate to model cosmic ray diffusion at those small scales, but not for the global diffusion. The exploration of these effects is one of the goals of our ongoing simulations of the ISM.

The expressions for the components of the cosmic-ray diffusion tensor obtained here are broadly consistent with the existing theoretical and computational results. The isotropic diffusion coefficient given by Equation (31) is the sum of an energy independent (for relativistic particles) and a Bohm-like component. While previous test particle simulations have shown a Bohm-like scaling (e.g., Casse et al. 2001; Fatuzzo et al. 2010; Beresnyak et al. 2011), it has been suggested that this scaling only applies down to a certain value of $R_{\rm L}$ much smaller than $l_{\rm c}$. Here we have found, more precisely, that the scaling continues down to $R_{\rm L} \approx 2\pi/k_{\rm max}$, which seems reasonable. It is not immediately clear why the previous simulations are inconsistent with this result or how to obtain theoretically the energy-independent part of the diffusion coefficient. Some previous works (e.g., Globus et al. 2008; Harari et al. 2014) have fitted isotropic diffusion results by including the theoretically motivated quasilinear E^{2-s} term, equivalent to the $R_{\rm L}^{1/3}$ term in our parallel diffusion expression, Equation (23). Despite this difference, Equation (31) varies less than 15 per cent from the expression of Harari et al. (2014) for $l_{\rm c}/50 \lesssim R_{\rm L} < l_{\rm c}/2$, when $s = 5/3$. The parallel diffusion coefficient given by Equation (23) appears to be consistent with a quasilinear scaling at low η, while the simple addition of the isotropic diffusion coefficient compensates very well for the breakdown of this scaling at $\eta \to 1$. One should note that the quasilinear result of Equation (24) is based on an MHD wave propagation model in the limit of zero-frequency waves (Berezinskii et al. 1990; Aloisio & Berezinsky 2004), whereas a calculation more consistent with our underlying magnetic field model, i.e., magnetostatic turbulence, usually yields an infinite diffusion coefficient (Fisk et al. 1974). [This is a problem with the original quasilinear theory, relating to scattering at pitch angles of $\theta = \pi/2$. The problem might be overcome in several ways; see e.g. Cesarsky & Kulsrud (1973), Tautz et al. (2008)]. One explanation for this apparent good agreement with a slightly inconsistent theory might be that the effect of propagating MHD waves is not very important when considering asymptotic diffusion coefficients (Fatuzzo et al. 2010). And finally, the local perpendicular diffusivity $\kappa_\perp$ scales almost perfectly with the magnetic field line diffusion coefficient.

Regarding test particle simulations, we have shown that discrete and continuous magnetic field constructions can yield essentially identical results over a broad range of particle energies. For magnetic fields on a discrete mesh, our results suggest that caution is required when $R_{\rm L}$ is less than a few mesh points or is a significant fraction of L.

ACKNOWLEDGMENTS

AS and LFSR acknowledge useful discussions with the members of the International Team 323 of the International Space Science Institute in Bern. Useful comments of Diego Harari are gratefully acknowledged. APS would like to thank David Ruffolo and Wirin Sonsrettee for useful discussions. APS is grateful to the School of Mathematics and Statistics in Newcastle for hospitality. This work was supported by the Leverhulme Trust (Grant RPG-2014-427) and the STFC (Grant ST/L005549/1).

REFERENCES

Akahori T., Ryu D., 2011, ApJ, 738, 134
Aloisio R., Berezinsky V., 2004, ApJ, 612, 900
Armstrong J. W., Rickett B. J., Spangler S. R., 1995, ApJ, 443, 209
Bakunin O. G., 2008, Turbulence and Diffusion: Scaling Versus Equations. Springer, Berlin
Batchelor G. K., 1953, The Theory of Homogeneous Turbulence. Cambridge University Press
Beck R., Brandenburg A., Moss D., Shukurov A., Sokoloff D., 1996, ARA&A, 34, 155
Beck R., Shukurov A., Sokoloff D., Wielebinski R., 2003, A&A, 411, 99
Beresnyak A., Yan H., Lazarian A., 2011, ApJ, 728, 60
Berezinskii V. S., Bulanov S. V., Dogiel V. A., Ptuskin V. S., 1990, Astrophysics of Cosmic Rays. North-Holland, Amsterdam
Boris J. P., 1970, in Proceedings of the Fourth Conference on Numerical Simulation of Plasmas. Naval Res. Lab., Washington, D.C, pp 3–76
Candia J., Roulet E., 2004, J. Cosmology Astropart. Phys., 10, 7
Cash J. R., Karp A. H., 1990, ACM Trans. Math. Softw., 16, 201
Casse F., Lemoine M., Pelletier G., 2001, Phys. Rev. D, 65, 023002
Cesarsky C. J., Kulsrud R. M., 1973, ApJ, 185, 153
De Marco D., Blasi P., Stanev T., 2007, J. Cosmology Astropart. Phys., 6, 27
Evoli C., Gaggero D., Grasso D., Maccione L., 2008, J. Cosmology Astropart. Phys., 10, 18
Farge M., Schneider K., 2015, J. Plasma Phys., 81, 43
Fatuzzo M., Melia F., Todd E., Adams F. C., 2010, ApJ, 725, 515
Fisk L. A., Goldstein M. L., Klimas A. J., Sandri G., 1974, ApJ, 190, 417
Fletcher A., Shukurov A., 2007, in Miville-Deschênes M.-A., Boulanger F., eds, EAS Publ. Ser. Vol. 23, Sky Polarisation at Far-Infrared to Radio Wavelengths: The Galactic Screen before the Cosmic Microwave Background. pp 109–128 (arXiv:astro-ph/0602536)
Fung J. C. H., Hunt J. C. R., Malik N. A., Perkins R. J., 1992, J. Fluid Mech., 236, 281
Gaggero D., Maccione L., Di Bernardo G., Evoli C., Grasso D., 2013, Phys. Rev. Lett., 111, 021102
Gent F. A., Shukurov A., Sarson G. R., Fletcher A., Mantere M. J., 2013, MNRAS, 430, L40
Giacalone J., Jokipii J. R., 1994, ApJ, 430, L137
Giacalone J., Jokipii J. R., 1999, ApJ, 520, 204
Globus N., Allard D., Parizot E., 2008, A&A, 479, 97
Goldstein M. L., Roberts D. A., Matthaeus W. H., 1995, ARA&A, 33, 283
Green M. S., 1951, J. Chem. Phys., 19, 1036
Hanasz M., Wóltański D., Kowalik K., 2009, ApJ, 706, L155
Harari D., Mollerach S., Roulet E., 2014, Phys. Rev. D, 89, 123001
Haverkorn M., Brown J. C., Gaensler B. M., McClure-Griffiths N. M., 2008, ApJ, 680, 362
Howes G. G., 2015, Phil. Trans. R. Soc. A, 373, 40145
Iacobelli M., et al., 2013, A&A, 558, A72
Jokipii J. R., 1966, ApJ, 146, 480

Jokipii J. R., Parker E. N., 1968, Physical Review Letters, 21, 44
Kóta J., Jokipii J. R., 2000, ApJ, 531, 1067
Kubo R., 1957, J. Phys. Soc. Japan, 12, 570
Kulsrud R. M., 2004, Plasma Physics for Astrophysics. Princeton. Univ. Press, Princeton
Maccione L., 2013, Phys. Rev. Lett., 110, 081101
Mace R. L., Dalena S., Matthaeus W. H., 2012, Physics of Plasmas, 19, 032309
Michalek G., Ostrowski M., 1997, A&A, 326, 793
Miniati F., 2001, Computer Phys. Comm., 141, 17
Miniati F., 2007, J. Computational Phys., 227, 776
Minter A. H., Spangler S. R., 1996, ApJ, 458, 194
Monin A. S., Yaglom A. M., 1975, Statistical Fluid Mechanics, Vol. 2. MIT press, Cambridge, MA
Parizot E., 2004, Nuclear Phys. B, Proceedings Suppl., 136, 169
Plotnikov I., Pelletier G., Lemoine M., 2011, A&A, 532, A68
Ruffolo D., Chuychai P., Wongpan P., Minnie J., Bieber J. W., Matthaeus W. H., 2008, ApJ, 686, 1231
Ruzmaikin A. A., Shukurov A. M., Sokoloff D. D., 1988, Magnetic Fields of Galaxies. Kluwer, Dordrecht
Schlickeiser R., 2002, Cosmic Ray Astrophysics. Springer, Berlin
Shalchi A., 2009, Nonlinear Cosmic Ray Diffusion Theories. Vol. 362, Springer, Berlin, doi:10.1007/978-3-642-00309-7
Shalchi A., 2011, Phys. Rev. E, 83, 046402
Shalchi A., Dosch A., 2009, Phys. Rev. D, 79, 083001
Shukurov A., 2007, in Dormy E., Soward A. M., eds, Mathematical Aspects of Natural Dynamos. Chapman & Hall/CRC, London, pp 313–359
Siejkowski H., Otmianowska-Mazur K., Soida M., Bomans D. J., Hanasz M., 2014, A&A, 562, A136
Snodin A. P., Brandenburg A., Mee A. J., Shukurov A., 2006, MNRAS, 373, 643
Snodin A. P., Ruffolo D., Matthaeus W. H., 2013, ApJ, 762, 66
Sonsrettee W., et al., 2015a, submitted to ApJS (Sept. 2015)
Sonsrettee W., Subedi P., Ruffolo D., Matthaeus W. H., Snodin A. P., Wongpan P., Chuychai P., 2015b, ApJ, 798, 59
Stepanov R., Shukurov A., Fletcher A., Beck R., La Porta L., Tabatabaei F., 2014, MNRAS, 437, 2201
Strong A. W., Moskalenko I. V., 2001, Adv. Space Res., 27, 717
Strong A. W., Moskalenko I. V., Ptuskin V. S., 2007, Ann. Rev. Nucl. Particle Sci., 57, 285
Tautz R. C., Shalchi A., Schlickeiser R., 2008, ApJ, 685, L165
Taylor G. I., 1922, Proc. London Math. Soc., s2-20, 196
Urch I. H., 1977, Ap&SS, 46, 389
Vladimirov A. E., et al., 2011, Computer Phys. Comm., 182, 1156
Wilkin S. L., Barenghi C. F., Shukurov A., 2007, Phys. Rev. Lett., 99, 134501
Zeldovich Y. B., Ruzmaikin A. A., Sokoloff D. D., 1990, The Almighty Chance. World Scientific Publication, Singapore

APPENDIX A: COMPARISON OF MAGNETIC FIELD MODELS AND RESOLUTION TESTS

First, for reference, Figure A1 compares the time evolution of κ_0 given by Equation (17) at various values of $R_{\rm L}$. For $l_{\rm c}/8 \leq R_{\rm L} \leq 2l_{\rm c}$, the subdiffusive regime is rather short (about ten time units) and the diffusivity quickly reaches an asymptotic value. For $R_{\rm L} \gg l_{\rm c}$, both the diffusion coefficients and the time required to reach the diffusive propagation can be very large. With open circles, for some values of $R_{\rm L}$, we have also plotted in Figure A1 the usual asymptotic diffusion coefficient as given by Equation (18), evaluated after various times. It is clear that it is consistent with the running diffusion coefficient at large times. However, the running diffusion coefficient converges at much earlier time, so is therefore more appropriate for practical evaluation. This is because the running diffusion coefficient depends on the local (in time) change in the particle mean squared displacement, whereas Equation (18) is a global average and must be evaluated at large times in order to forget the initial evolution.

To understand the advantages and limitations of the two models of a random magnetic field and to estimate the numerical resolution required to achieve a desired accuracy, we compare the diffusion coefficients obtained with the two models. One might expect that the main deficiency of the magnetic field constructions will be an insufficient number of modes near the scale $k_{\rm res} = 2\pi/R_{\rm L}$, which would likely result in lower than expected levels of scattering. Thus, we consider a few values of $R_{\rm L}$ and a purely random magnetic field, $\eta = 1$. Both theory and earlier numerical results suggest different regimes of diffusion for the cases $R_{\rm L} \ll l_{\rm c}$ and $R_{\rm L} \gg l_{\rm c}$, so we consider the cases $R_{\rm L} = 5l_{\rm c}$, $l_{\rm c}$ and $l_{\rm c}/5$, where $l_{\rm c}$ is obtained from Equation (7). Figure A2 shows the running isotropic diffusion coefficient $\kappa_0 = (1/3)\sum_{i=1}^{3}\kappa_{ii}$ for $s = 5/3$. We focus on the time intervals where differences between the two models are the strongest, so that the relative differences between the various lines are far larger in Panel (a) than in (b). Note that here it is necessary to have very good particle statistics so that we can attribute differences in the diffusion coefficients to changes in the magnetic field resolutions, rather than the statistical error in the evaluation of a diffusion coefficient; we estimate the maximum relative standard error in the diffusion coefficients to be less than 1 per cent in all cases.

For $R_{\rm L} = 5\,l_{\rm c}$ (Figure A2a), the cosmic rays become diffusive at $t \approx 30\,t_0$. In this regime, convergence of the diffusion coefficients in a continuous magnetic field seems to require a large number of modes N per unit of $k_{\rm max}/k_0$ when compared with the other panels at lower $R_{\rm L}$. On the other hand, large values of $k_{\rm max}/k_0$ may not be required because the particles are not dominated by magnetic fields at small scales for a sufficiently steep magnetic spectrum. Plotnikov et al. (2011) conclude that $k_{\rm max}/k_0 = 10$ is adequate for large $R_{\rm L}$. For $k_{\rm max}/k_0 = 96$, the choices $N = 150$ and 600 lead to a difference of more than 10 per cent in the diffusivity. For $N = 512$ and $k_{\rm max}/k_0 = 256$, we might expect the diffusion coefficient to be smaller than with $N = 600$ since the correlation length is smaller (according to the restricted k evaluation of Equation 7). However, the mode density seems to be too low to realise this with $N = 512$, but taking $N = 1024$ is sufficient to give the expected result. For a given $k_{\rm max}/k_0$, we find that the diffusion coefficients always decrease with increasing N. Whereas the continuum model concentrates modes near k_0,

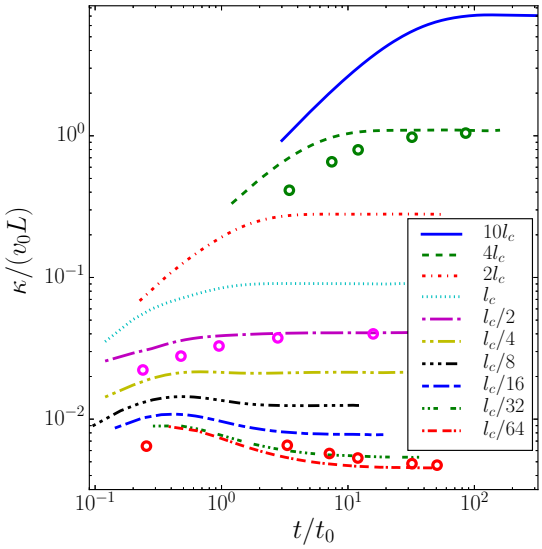

Figure A1. Time evolution of the (isotropic) running diffusion coefficient for vanishing mean field, $B_0 = 0$, for various values of $R_{\rm L}$ as specified in the legend. The continuous magnetic field model has been used with $N = 512$ and $k_{\rm max}/k_0 = 256$. In the case of $R_{\rm L} = 4l_{\rm c}, l_{\rm c}/2$ and $l_{\rm c}/64$, open circles show the evaluation of the usual asymptotic diffusion coefficient, i.e. Equation (18), after time t/t_0. We see that this is consistent with the running diffusion coefficient if evaluated at sufficiently large time. However, for practical evaluation of the diffusion coefficients, clearly the running diffusion coefficient is preferable, since it converges at much earlier time.

the discrete model has very few modes at low k, which is perhaps why we see a large discrepancy between the 512^3 resolution discrete model and the continuous ones in Panel (a). By increasing both the mesh separation corresponding to wave number k_0 and the overall mesh size (denoted by a star in the figure legend), it appears that this discrepancy can be eliminated. We tried increasing the resolution alone, up to 1600^3, but this had little effect.

In Panel (b), for $R_\mathrm{L} = l_\mathrm{c}$, too few modes in the continuous model of Equation (9) appear to cause a problem. Overall though, there is less variation in the asymptotic κ between various resolutions than in Panel (a). With the resolution 1024^3 in the discrete magnetic field model and $N > 150$ in the continuous model, the asymptotic diffusivities agree within about 2 percent over the whole time evolution (although the $N = 600$ case turns out to be somewhat special, leading to a lower value of κ than for the other values of N). It is also quite satisfactory that significant variation in the resolution of the discrete model does not affect the result much.

The difference between results obtained under the whole range of magnetic field implementations is even smaller in Panel (c), for $R_\mathrm{L} = l_\mathrm{c}/5$. The diffusivities in the three continuous models coincide almost perfectly, which suggests we have sufficient resonant scattering. It is perhaps surprising that although the discrete model contains many more modes near k_res than the continuous one, it seems to require that k_max be several times larger than k_res for convergence, whereas the continuous one is well converged at $k_\mathrm{max} \approx k_\mathrm{res}$. This may be due to the discrete nature of the model and is discussed further in Section 3.

The results here suggest that the two models will be in almost perfect agreement in the limit of high resolution and when k_0 is sufficiently well resolved in the discrete model. Clearly the discrete model is more limited in the range of R_L that can be considered and presumably the limitations mentioned above will apply to test particle simulations in more realistic magnetic fields. For the range of R_L studied, we see no obvious effects due to the periodic magnetic field. For continuous magnetic field models, some previous works have determined reasonable values of N for particular cases, which has typically been quantified in terms of the number of modes A required per decade of k_max/k_0, i.e. $N = A \log_{10}[k_\mathrm{max}/k_0]$. Examples of reported reasonable values of A are 25 (Fatuzzo et al. 2010), 100 (Parizot 2004), and 200–300 (Plotnikov et al. 2011). Considering the results of figure A2, $A = 25$ might be reasonable for $R_\mathrm{L} = l_\mathrm{c}/5$. However, for $R_\mathrm{L} = 5l_\mathrm{c}$ this would give $N \approx 50$ for $k_\mathrm{max}/k_0 = 96$, which would appear to be unreasonably small. Our results for $N = 512, k_\mathrm{max}/k_0 = 256$ seem reasonable over all panels, and this gives $A \approx 213$, which is of similar size to those previously reported. The point to note here is that a given reasonable value of A is not universally applicable and will depend on both R_L and the desired range k_max/k_0.

Admittedly we have not performed such a detailed study of the convergence for $\eta < 1$. However, for some values of η, and at the extremes of R_L, we have observed similar asymptotic trends to those discussed above and in Section 3, so we suspect that variation of η is not a very important consideration, except perhaps in the limit $\eta \to 0$.

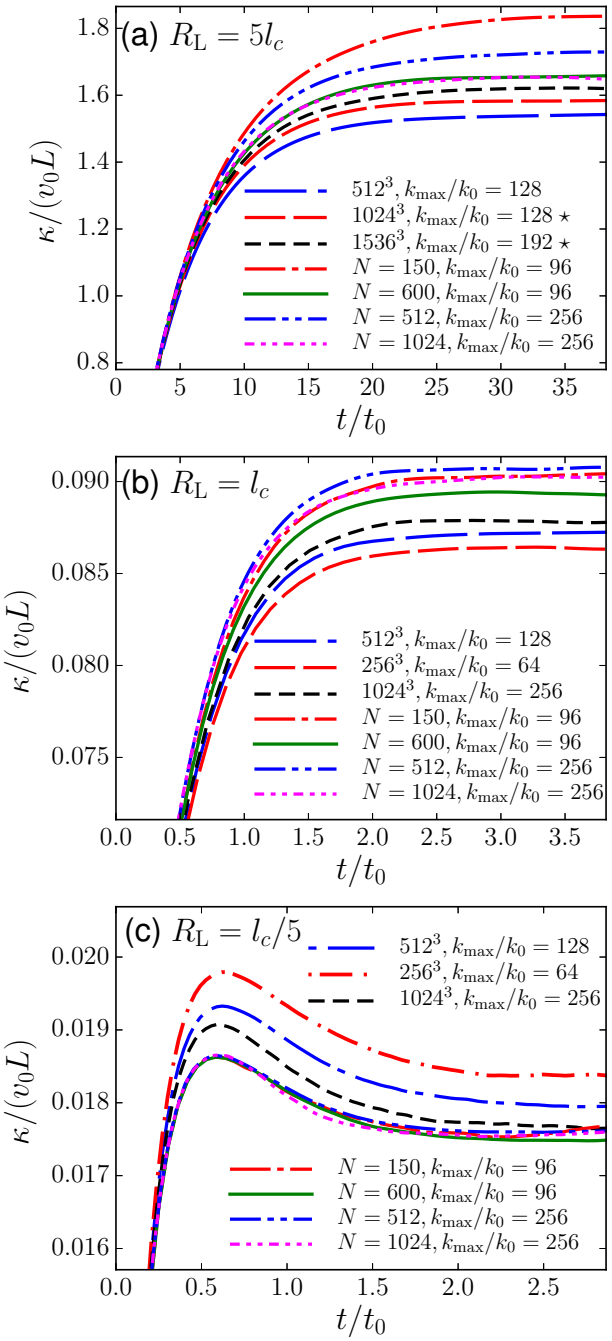

Figure A2. A comparison of the running diffusion coefficient obtained for the continuous and discrete magnetic field models under various numerical resolutions in k-space, specified in the legends, for $s = 5/3$ and a purely random magnetic field, $B_0 = 0$, at various values of R_L: (a) $R_\mathrm{L} = 5l_\mathrm{c}$; (b) $R_\mathrm{L} = l_\mathrm{c}$ and (c) $R_\mathrm{L} = l_\mathrm{c}/5$. For the discrete model (12), k_0 is taken to be equal to two mesh separations in wave number space (see page 4), apart from the two cases denoted with a star in Panel (a), for which k_0 is equal to four mesh separations.